Motion detection, labeling, data association and tracking, in real-time on RISC computer

Lionel Lacassagne[1,2], Maurice Milgram[1], Patrick Garda[1]
[1]Laboratoire des Instruments et Systèmes
Université Pierre et Marie Curie BC 252
4 place Jussieu, 75252 Paris - FRANCE
lionel | garda@lis.jussieu.fr maum@ccr.jussieu.fr
[2]IMASYS
Le quadral 23 bis rue E. Nieuport
92150 Suresnes - FRANCE

lionel@imasys.fr

Abstract - **This article introduces somes algorithms for motion detection and tracking. To be able to track moving objects, the analysis rate must be fast enough in order to keep the considered movements slow (and the features of the objects not changing too fast). We are presenting a Markov Random Field based motion detection algorithm running in real time on Pentium II and DSP C6x. For the medium level, we have developed a fast labeling algorithm, a benchmark is provided. The high level is fast because the previous processing steps are running at a faster rate than the video rate.**

I. Motion Detection

The motion detection (MD) is the base of all systems for trackings object and image compression. The MD algorithms are mainly belonging to two classes: optical flow and correlation. These methods have been widely explored, everyone of them has some advantages and drawbacks. The simplest method is an image difference, where a significant variation of the grey level is associated to a movement.

At the same time, Markov Random Field based algorithms have assert themselves in a lot of image processing areas for regularising ill posed problems(edge detection, region segmentation, restoration)[6]. If their main advantage is the robustness, their main drawback is their CPU consumming due to the huge amount of calculations. This leads researchers to study a lot of solutions to speed their execution up, as Parallel Machine, or dedicated architecture [2][1][5]. We describe the use of MRF for enhancing an image difference. After explaining the different kinds of optimizations, we show how to reach real time on RISC and DSP.

A. A MRF approach

The aim of the markovian process is to improve the quality of the image difference with a relaxation algorithm. Because of changes of illumination, this image is very noisy: a lot of pixels are labelled as in motion and the regions are not filled. The energy model has been introduced by the Lis-Grenoble lab [3][4].

Let I_t, be the grey level image at the moment t, and O_t the observation ($O_t = |I_t - I_{t-1}|$). Then thresholding O_t initializes the estimated field of label $\hat{E}_t$. The background/movement sites are labeled 0/1. The Iterated Conditional Modes (ICM fig1) is then applied to find the relaxed label field E_{t-1} from $\hat{E}_t$, $\hat{E}_{t-1}$ and E_{t-2}. Relaxation being deterministic, the algorithm converges in few iterations (fixed to four), to the first local minimum, so the initialization is very important. The straight forward image difference may be enhanced by a maximum likelihood [7], with or without confidence (CPU expensive).

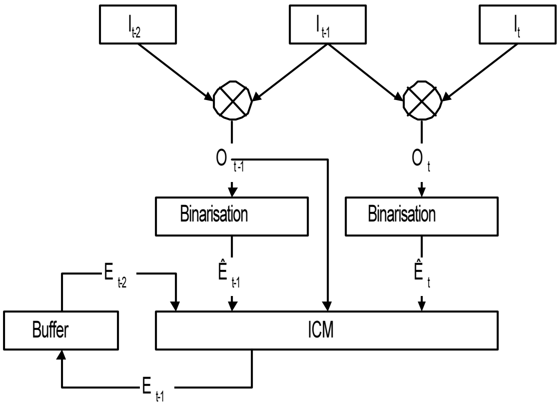

Figure 1 – Relaxation algorithm

B. Energy function, clique.

The energy model u used is the sum of two energies: u_m model energy that is a regulation term which ensures a spatiotemporal homogeneity and which also expresses the relation with the neighboring sites, and u_a adequation energy which prevents the model to drift too far from the initialization.

$u(o_s, e_s) = u_m(e_s) + u_a(o_s, e_s)$

$u_m(e_s) = \sum_{c \in C} V_c(e_s, e_r)$

$u_a(o_s, e_s) = \frac{1}{2\sigma^2}\left[o_s - \Psi(e_s)\right]^2$

$\Psi(e_s) = \begin{cases} 0 & \text{if background} \\ \alpha > 0 & \text{if mouvement} \end{cases}$

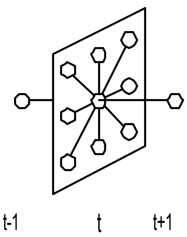

Figure 2 – spatio-temporal clique

Clique associated to u_m energy is a spatiotemporal and second order clique (Fig 2). The spatial potential function V_s is:

$V_c(e_s, e_r) = V_s(e_s, e_r) + V_p(e_s^t, e_s^{t-1}) + V_f(e_s^t, e_s^{t+1})$

$V_s(e_s, e_r) = \begin{cases} -\beta_s & \text{if} \quad e_s = e_r \\ +\beta_s & \text{if} \quad e_s \neq e_r \end{cases}$

The temporal potentials V_p and V_f, associated to the past and future cliques are:

$V_p(e_s^t, e_s^{t-1}) = \begin{cases} -\beta_p & \text{if} \quad e_s^t = e_s^{t-1} \\ +\beta_p & \text{if} \quad e_s^t \neq e_s^{t-1} \end{cases}$

$V_f(e_s^t, e_s^{t+1}) = \begin{cases} -\beta_f & \text{if} \quad e_s^t = e_s^{t+1} \\ +\beta_f & \text{if} \quad e_s^t \neq e_s^{t+1} \end{cases}$

With the Ising model (spin up/spin down : +1/-1):

$u_m = -\beta_s \sum_{c \in C} x_s^t x_r^t - \beta_p x_s^t x_s^{t-1} - \beta_f x_s^t x_s^{t+1}$

with x_s^t, the spin of the site x, at t.

In order to make the trace of I_{t-1} to disappear, and to fill the overlapping, area due to the image difference, it is convenient to respect the inequality:

$\beta_p < \beta_s < \beta_f$

Experimental tests demonstrate that the required parameters (β_p, β_s, β_f, α) do not have to be tuned according to the image sequence. They are set to the values:

$\beta_p = 10, \beta_s = 20, \beta_f = 30, \alpha = 20$

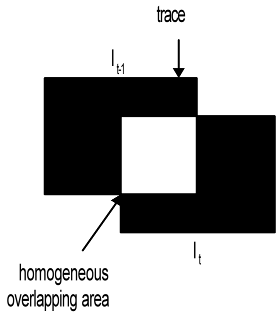

Figure 3 – $O_t = |I_t - I_{t-1}|$

C. Optimization

1. The optimizations techniques

The most common used technique is the 'loop-unrolling' (LU). It consists in the duplication of the loop body, but also, when it is possible to make some computation in 'parallel'. Even so, the C6x pipeline is not always full. The software pipelining (SP) can solve this problem by maximizing the use of the different units.

2. Algorithm characteristics

Two consecutive masks overlap on two columns. So the computation of the spatial energy is then split-up in three columns, and only one new column is computed instead of the three previously required. The entire computation is performed by Look-Up

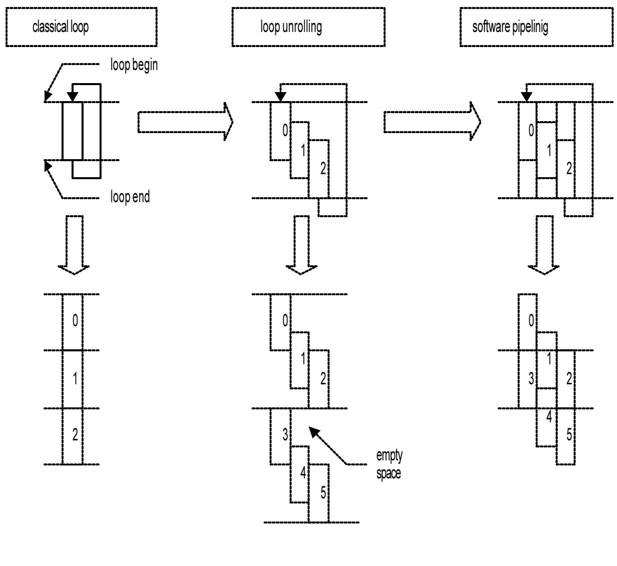

Figure 4 – loop-unrolling, software pipelining

Tables (LUT) to avoid CPU intensive multiplications.

The background/movement sites are labeled 0/1 rather than −1/1. Instead of comparing the state of each site to the central site e_s, we just take into account sites which state are 1 (p_1, s_1 and f_1 for the past, present and future images). So if the central site state is 1 the spatial energy is:

$u_{m1} = (8-2s_1)\beta_s + (1-2p_1)\beta_p + (1-2f_1)\beta_f$, else $u_{m0} = -u_{m1}$

If $u_{m1} + u_{a1} < u_{m0} + u_{a0}$, the state is set to 1 otherwise it is set to 0. The change is performed whatever the previous state is. The test can be simplified by factoring the model and adequation terms: $2u_{m1} < u_{a0} - u_{a1} = \frac{\alpha}{2\sigma^2}(2o_s - \alpha)$. This a priori minor modification can save 1 cycle on a total of 6 on DSP C6x, that is to say 17%!

3. Implemented optimizations

The algorithm has been implemented on a Pentium II 400 MHz, and has been estimated (from the number of cycles of the loop) for the TI-C6202 at 250 MHz. On the Pentium the number of available registers is insufficient to perform the Loop-Unrolling. So this is the 8-accesses-per-point version, but with a LUT, that has been implemented. On the C6x there are enough registers. A Loop-Unrolling of order 3 is performed. Because the model energy is computed faster with multiplications (4 cyles) than with LUT (5 cycles) we use multiplications for u_m and LUT for u_a. The figure 5 gives the scheduling on a C6x (the indexes correspond to the delay with the current index t).

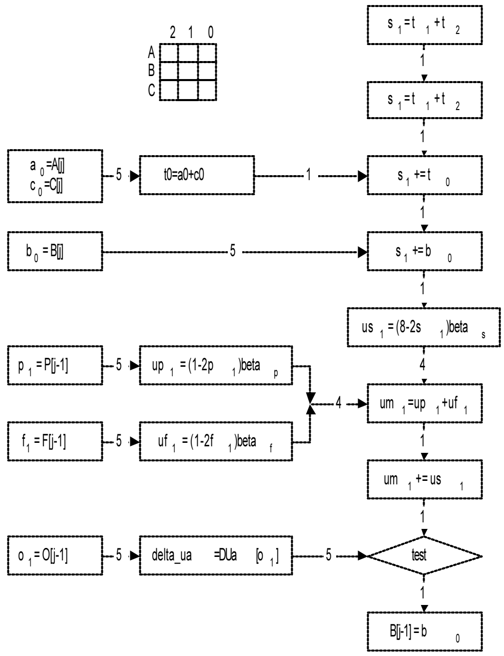

Figure 5 – C6x scheduling

Per point, and on a C6202, the estimated time, depending on the performed optimizations (none, Loop-Unrolling, or Software Pipelining) are:

optimization techniques	none	LU	SP
instructions	22	66	66
cycles	15	25	15
ipc	1.47	2.64	4.40
% charge	15	26	44
MIPS	367	660	1100

A comparison of the different architectures implementing the ICM relaxation is given in the figure 6. Standard RISC processors, programmed in C, achieve real time execution for image size larger than 256^2 (up to 320^2), and fixed point DSP, in assembly language for image size larger than 512^2 (up to 700^2).

II. Light Speed Labeling: a fast and new algorithm

This paragraph introduces a fast algorithm for labelling binary images.Its speed is almost independant from data. Moreover its structure makes the 8-connected version as fast as the 4-connected ver-

Labs	Architechture	# chips	f(MHz)	image size	rate
Lis Grenoble	CNAPS	256	20	128^2	3
Lis Grenoble	M 96002	1	40	128^2	15
Lasmea	Transvision (T9000)	8	50	$\sim 256^2$ (350x188)	11
Lis Paris	C80	1+4	60	256^2	18
Lis Paris	Pentium II	1	400	256^2	40
Lis Paris	C6202 (simulation)	1	250	512^2	47

Figure 6 – different implementations

sion. The proposed algorithm is optimum with the number of created labels, and it can be easily and efficiently parallelized.

A. *Classic labeling, RLC-based labeling*

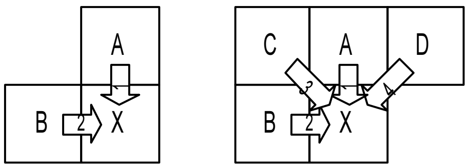

Figure 7 – 4 and 8-connected neighbors labeling

Standard algorithms use either the pixel approach (Fig 7: comparison of the current label, with the neighboring pixels) or the Run Length Coding (search for an adjacent segment in order to find out the connectivity). Both of them involve a great amount of tests, and, at the CPU level this leads to many pipeline stalls (waiste of time) because the test result is, of course, unpredictible. Lastly and it is not its least drawback, the pixel labeling produces many useless labels.

B. *LSL algorithm*

The main idea in LSL is to replace all the tests (label comparisons, fusion sort for segment intersection) by a set of simple instructions without (or with much less) tests. These instructions are fast because pipelinable.

The speed of LSL is based on 3 key points:

- intensive use of RLC
- introduction of "relative" and "absolute" labels for a direct access (LUT) to the label of the intersected segments
- a cyclic implementation of equivalences instead of a "flat" implementation.

Here are the differents steps of the algorithm. The explanations will be illustrated by the example of the figure 8.

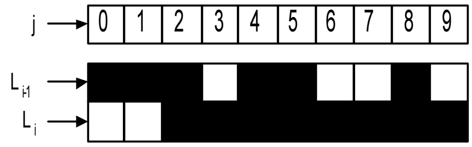

Figure 8 – Lines L_i, L_{i-1}

1. Computation of ER_i and RLC_i

j	0	1	2	3	4	5	6	7	8	9
ER_{i-1}	1	1	1	2	3	3	4	4	5	6
ER_i	0	0	1	1	1	1	1	1	1	1

Figure 9 – table ER

The ER_i table holds, for each line L_i, the associated relative label e_r of each segment (object with an *odd* number) and each non-segment (background with an *even* number).

RLC_{i-1}	0	2	4	5	8	8
RLC_i	2	9				

Figure 10 – table RLC

The RLC_i table holds the "begin" and "end" indexes of each segment $[a..b]$. The $j-th$ segment of relative label $e_r = 2j+1$ has the boundaries $a = RLC_i[2j]$, $b = RLC_i[2j+1]$. The current segment has an intersection with the segments numbered $e_{r0} = ER_{i-1}[a]$ $e_{r1} = ER_{i-1}[b]$. The labels e_{r0} / e_{r1} are enventually adjusted to point to the next / previous segment and not to the background:

To perform a 8-connected labeling, which is equivalent to test the diagonal labels (NW, NE), it is enough to increment a by 1 and to decrement b by 1, just before looking up the ER_{i-1} table. That makes the 8-connected version as fast as the 4-connected version.

2. Computation of ERA_i

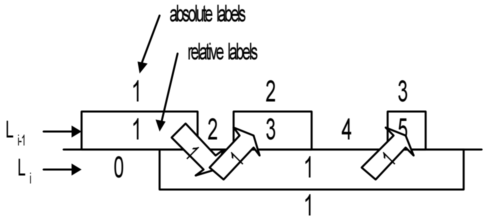

Figure 11 – absolute and relative labels

The ERA_i associates the relative and absolute label of a line. The table is calculated during the top-down labels propagation. The relative label is associated with the absolute label of the first intersected segment:

$$e_r = 1$$
$$\begin{cases} a = RLC_i[0] = 2 \Rightarrow a = 1 \\ b = RLC_i[1] = 9 \Rightarrow b = 9 \end{cases} \begin{cases} e_{r0} = 1 \\ e_{r1} = 6 \Rightarrow e_{r1} = 5 \end{cases}$$
$$e_a = ERA_{i-1}(e_{r0}) = 1 \text{ , } ERA_i(e_r) = e_a$$

3. Computation of EQ

To solve equivalence problems (computing the transitive closing of a graph is a complex problem) like adding an item to a class, or more generally to fusion two classes, the equivalence classes have been implemented with cyclic graphs in the EQ table.

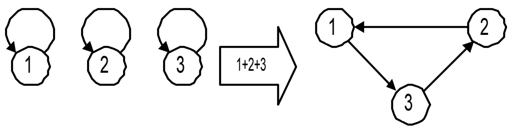

Figure 12 – equivalence cycle

During the fusion, e_a,must be associated with the other absolute labels e_{ak} of the intersected labels.

$e_{rk} \in [e_{r0} + 2..e_{r1}]$, $e_{ak} = ERA_{i-1}[e_{rk}]$

$fusion(e_a, e_{ak})$

with the example of the previous section:

$e_{rk} \in [e_{r0} + 2..e_{r1}]$

$e_{rk} \in \{3, 5\}$, $e_{ak} \in \{2, 3\}$

for the absolute labels, we have the equivalences.

The equivalence of the 3 labels will be processed like in figure 12.

4. Computation of EA_i

The absolutes labels of Li are obtained by LUT:

$EA_i = ERA_i(ER_i)$

5. Packing labels and relabeling

At the end, labels are packed (to get continuous number) from EQ to A. The whole image is then updated: $EA_i = A(EA_i)$

C. Benchmark of LSL

The algorithm has been compare to classic pixel based algorithm, eventually enhanced by cyclic equivalence. All versions use 16-bit labels. LSL is also implemented in 8-bit because sometime the number of labels is inferior to 256. We tested the algorithms on 4 cases of labeling : small/big regions few/many characters. We give the results in ms for 4-connected and 8-connected versions. The image size is 512×512.

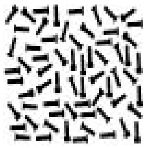

bolts

logo

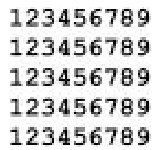

caps72

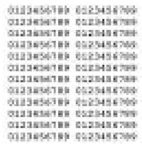

caps28

	bolts		logo	
	4C	8C	4C	8C
pixel	32	64	26	50
pixel+cycle	20	24	68	42
LSL 16bit	21	21	20	20
LSL 8bit	12	12	11	11
LSL vs pixel gain	2.7	5.3	2.4	3.7

	caps 72		caps 28	
	4C	8C	4C	8C
pixel	20	30	20	30
pixel+cycle	24	20	19	23
LSL 16bit	20	20	23	23
LSL 8bit	12	12	-	-
LSL vs pixel gain	1.7	2.5	0.9	1.4

Our algorithm outperforms by a factor from 2.4 to 5.3 pixel-labeling for the type of image used in real motion detection. Even for OCR, LSL is a bit faster.

III. Region matching

The matching system remains simple. It can not track neither two crossing regions, nor manage an object splitted into many regions. But it is fast and it will be the base to compare to clever systems using artificial intelligence [8].

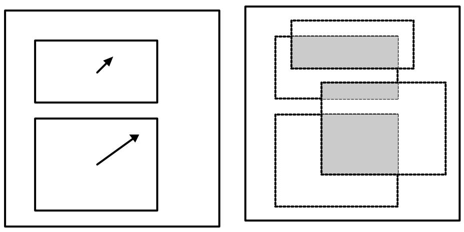

I_{t-1} I_t

For two consecutive images (I_{t-1}, I_t), the intersection area is computed (in grey on the Fig I_t). for each region these surfaces are sorted into descending numerical order. Associating labels is then equivalent to search the best matching all over the tree. In this tree a node corresponds to a specific matching between two regions of two consecutive images, and a branch corresponds to a set of matchings. The chosen sub-tree is this which maximizes the sum of the intersected surfaces. Thanks to the sort, the best sub-tree is located on the left of the tree, even it is the leftiest sub-tree of the tree.

The following images are extracted from the famous "taxi" sequence. Figures I_3 and I_4 are the original images, figures $\hat{E}_3$, $\hat{E}_4$ are the absolute difference O_t binarized with a threshold value of 5, and figures E_3, E_4 are the ICM relaxed images.

I_3

I_4

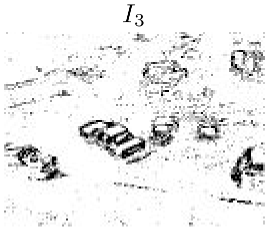

$\hat{E}_3$

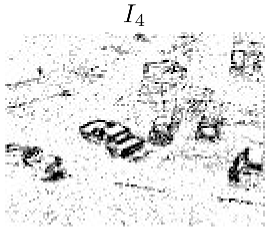

$\hat{E}_4$

E_3

E_4

IV. Conclusion

In this article, we have shown how to get a real time and a robust motion detection based on MRF on a RISC and DSP. We have proposed an new labeling algorithm, faster than the classical ones. Then, because these algorithms are fast and because we get good results, it remains enough time to perform a region matching and a tracking. Because all of these algoritms have been optimized, the whole processing is running in real time, at the video rate for 256×256 images.

References

[1] R. Azencott "Simulated annealing: parallelization techniques" John Whiley 1992

[2] A. Bellon "Détection et suivi de véhicule en mouvement, implémentation parallèle sur un système expérimental à mémoire distribuée", thèse LASMEA, Clermont Ferrand, Oct 1997.

[3] A. Caplier "Modèles markoviens de détection de mouvements dans les séquences d'images: approche spatio-temporelle, mise en oeuvre temps réel" thèse INPG, Grenoble 1995.

[4] A. Caplier, F. Luthon, C. Dumontier "Algorithmes markoviens de détection de mouvement, mise en oeuvre temps réel" GRETSI 1995.

[5] J.P. Cocquerez, S. Philipps "Analyse d'images: filtrage et segmentation", Masson 1995. Temps de calcul sur Sparc5 et CM2 (INRIA-Sophia), p220.

[6] F. Heitz, P. Bouthémy "Multimodal estimation of discontinuous optical flow using MRF" IEEE, Trans. on PAMI-15, N-12, Dec 1993.

[7] Y.Z. Hsu, H.H. Nagel, G. Rekers "New likelihood test methods for change detection in image sequences" CVGIP 26, 73-106, 1984

[8] P.H. Winston "Artificial Intelligence" Adison-Wesley, 1984